

MAGNETIC SPECTRA ANALYSIS OF DIELECTRICS

Jozef Sláma* – Martin Šoka* – Anna Grusková* – Vladimír Jančárik*
– Vladimír Ďurman* – Peter Široký** – Rastislav Dosoudil*

Method of dielectric and magnetic spectroscopy is used to analyze and interpret the spectra obtained by measurement of complex permittivity of $Ba_{1-x}Sr_x$ ferrites and permeability of substituted Ni ferrite and NiZn ferritepolymers. Ferritepolymers were prepared from NiZn ferrite particles dispersed in PVC polymer matrix. Effect of the filler content on the $\mu^*(f)$ spectra of NiZn ferritepolymers was examined and discussed from point of view the magnetization processed in samples. In $Ba_{0.25}Sr_{0.75}$ ferrite was finding two dielectric dispersion and absorption permittivity behavior as suggested by Maxwell-Wagner effect.

Key words: permeability, permittivity, ferrite, ferritepolymer

1 INTRODUCTION

In this time ferrites present specific qualities which not only allow the investigations of the magnetization processes, but have permitted some fundamental laws to be established in this field. Ferrites crystalline structure based on oxygen sublattice makes the material harder, so the samples are less sensitive to the whole history (treatment) of preparation. The ionic and granular structures lead to a lower conductivity which permits the material to be investigated easily up to high frequencies [1-4]. Therefore, magnetic or dielectric spectroscopy is powerful technique for estimation the material in a wide frequency range application and they are one of tool study of magnetization or ion transport mechanisms in the materials. In general, using the magnetic spectra, *ie* frequency dependence of complex permeability $\mu^*(\omega) = \mu'(\omega) - j\mu''(\omega)$, we can study various mechanisms of magnetization. Using the dielectric spectra frequency behaviour of complex permittivity $\varepsilon^*(\omega) = \varepsilon'(\omega) - j\varepsilon''(\omega)$ we can study molecular and ionic dynamics of charge carriers and dipoles. The dielectric spectra of prepared $Ba_{0.25}Sr_{0.75}Fe_{12}O_{19}$ hexaferrite were measured in range of 42 Hz to 2 MHz. The magnetic spectra of prepared ferrites were measured and estimated in frequency range of 1 MHz - 3 GHz using impedance spectroscopy. Method of magnetic spectroscopy is used to interpret and to analyze the experimental data obtained by measurement of the complex permeability of substituted Ni ferrites and ferritepolymers. In addition, the spectra of sintered ferrites with prepared ferritepolymer composites are compared from point of view the actual magnetization mechanism in presented samples.

2 DIELECTRIC SPECTROSCOPY OF FERRITE

The dielectrics measurement was carried out in $Ba_{1-x}Sr_x$ ferrite samples to show the spectra analysis. The dielectric parameter of the ferrite samples measured by an impedance analyzer were processed in the form of the complex permittivity $\varepsilon^*(f)$. The permittivity can be approximated by the locus diagram in the complex plane

where the real part $\varepsilon'(f)$ of the complex permittivity is plotted against the imaginary component $\varepsilon''(f)$.

Considerable change in dielectric permittivity was observed for different compositions of $Ba_{1-x}Sr_x$ ferrite. These variations of composition produce changes of $\varepsilon^*(f)$ pattern in complex plane. The two form $\varepsilon^*(f)$ of the sintered samples of $Ba_{1-x}Sr_x$ with different compositions are plotted as frequency spectra in Fig. 1 and 2 for example. The frequency dependence of $\varepsilon^*(f)$ for $Ba_{0.5}Sr_{0.5}Fe_{12}O_{19}$ ferrite is shown in Fig. 1 and the one for $Ba_{0.25}Sr_{0.75}Fe_{12}O_{19}$ is shown in Fig. 2. The locus diagram $\varepsilon^*(f)$ in Fig. 1 indicates a presence of simple frequency spectra due to a relaxation effect. The observed variation in the permittivity with frequency can be explained using phenomenological dispersion theory. It can be expressed and fitted by the Cole-Cole relaxation formula

$$\varepsilon^*(f) = \varepsilon_\infty + \frac{\varepsilon_s - \varepsilon_\infty}{1 + (j2\pi fT)^v} \quad (1)$$

where $\varepsilon_\infty \approx 20$ is the nonrelaxation permittivity (when $f \rightarrow \infty$), $\varepsilon_s \approx 595$ is the static permittivity (when $f \rightarrow 0$), T is the relaxation time and $v \in (0,1)$ is the material dispersion parameter.

The locus diagram $\varepsilon^*(f)$ shown in Fig. 2 is determined by two polarization processes. The observed variation in $\varepsilon^*(f)$ with frequency can be explained as the total effect of two "layers" as suggested by Maxwell-Wagner effect. According dispersion theory, the permittivity behaviour is suggested by Maxwell-Wagner model. For this, two layers are formed probably by "well"-conducting grains and their boundaries which are poorly-conducting. In this sample the Argand diagram permittivity $\varepsilon^*(f)$ may be expressed by the relation formula

$$\varepsilon^* = \frac{\varepsilon_{s1} - \varepsilon_{\infty 1}}{1 + (2\pi fT_1)^{v_1}} + \frac{\varepsilon_{s2} + (\varepsilon_{\infty 1} - \varepsilon_{s2})}{1 + (2\pi fT_2)^{v_2}} \quad (2)$$

where $0.8 < v_1, v_2 < 1$ are the dispersion and T_1, T_2 are time constants of two relaxations: $\varepsilon_{s1} \approx 4800$, $\varepsilon_{s2} \approx 1650$, $\varepsilon_{\infty 1} \approx 110$, $\varepsilon_{\infty 2} = 0$. The evolution of the plot $\varepsilon^*(f)$ is identical to that of a Cole-Cole lots. First of them is

*Slovak University of Technology, Faculty of Electrical Engineering and Information Technology, Ilkovičova 3, 812 19 Bratislava, Slovakia; martin.soka@stuba.sk, ** Trenčín University of Alexander Dubček.

relevant for low frequency range up to nearly 4 kHz and second lot is dominant for higher frequencies over 4 kHz. We can admit idea to finding two dielectric dispersion and absorption in a sample of $\text{Ba}_{0.25}\text{Sr}_{0.75}$ ferrite.

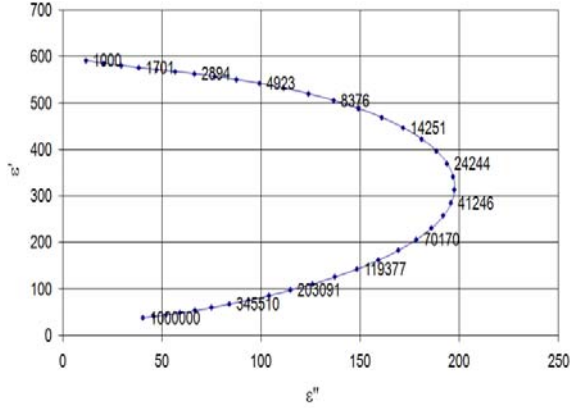


Fig. 1. Argand diagram of the complex permittivity for $\text{Ba}_{0.5}\text{Sr}_{0.5}\text{Fe}_{12}\text{O}_{19}$ at 67°C (the parameter is frequency in Hz)

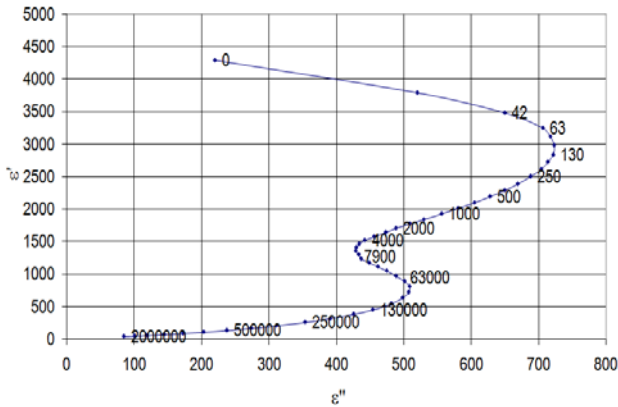


Fig. 2. Diagram of the complex permittivity for $\text{Ba}_{0.25}\text{Sr}_{0.75}\text{Fe}_{12}\text{O}_{19}$ at 66°C (the parameter is frequency)

If we will limit ourselves to the two layers model the common (typical) Maxwell – Wagner effect can be expressed as

$$\varepsilon' = \varepsilon_\infty + \frac{\varepsilon_s - \varepsilon_\infty}{1 + (2\pi f T_2)^2}, \quad \varepsilon'' = \frac{1}{2\pi f T_1} + \frac{\varepsilon_s - \varepsilon_\infty}{1 + (2\pi f T_2)^2} \quad (3)$$

In this typical case, the evolution of the plot $\varepsilon'(f)$ is identical to that of a Debye lot. In $\varepsilon''(f)$ the second term is identical to that of the Debye type, while the first term appears as supplementary term that carries with $1/2\pi f$. Therefore, when $f = 0$, plot $\varepsilon' \rightarrow \infty$. The evolution of the dielectric spectra of $\text{Ba}_{0.25}\text{Sr}_{0.75}$ samples measured at 21 and 35°C are looking like that, which corresponds to the relations (3). But difference is that the plot $\varepsilon'(f)$ is identical to that of a Cole-Cole lot. In $\varepsilon''(f)$ the second term is identical to that of the Cole-Cole type. It is probably caused by that the cation Ba^{2+} is substituting one of the O^{2-} anions in the layer of oxygen in the hexagonal structure. We have chosen the $\text{BaFe}_{12}\text{O}_{19}$ ferrite as an initial material, because ionic radius of Ba^{2+} cation (0.138 nm) is closest to ionic radius of O^{2-} (0.136 nm). Then, if

we will change the cation Sr^{2+} , having smaller ionic radius of 0.116 nm, for Ba^{2+} cation; in such case anions of O^{2-} which are placed in the sublattice 12k and 2b will be shifted in direction of layer with Ba^{2+} or Sr^{2+} ions. Simultaneously, arise to disorders in octahedrons O^{2-} of Fe^{3+} (12k) and Fe^{3+} (4f₂) ions; that manifests on change of value of anisotropy constant K . The gradient of electrical field around the nucleus will change and this will influence the interaction between quadrupole-moment of nucleus and gradient of electrical field. Probably for this reason there can be expected parallel polarization processes.

3 MAGNETIC SPECTROSCOPY OF FERRITES

Two magnetic dispersion and absorption were found in a sample of substituted Ni ferrite. The measured permeability spectra of sintered (at 1300°C) NiFe_2O_4 ferrite prepared by ceramic way with plausible permeability at low frequency is shown in Fig 3a. The real $\mu'(f)$ and imaginary $\mu''(f)$ component spectra are showing two well separated dispersions and absorptions. The first dispersion and absorption can be probably attributed to the wall motion and modeled similarly to the oscillation in the mechanical system. Hence, by analogy, the equation of domain wall motion can be derived. Based on this analogy, and under certain simplifying assumptions, the permeability spectra for d.w. motion can be expressed by the formula

$$\mu_d^*(\omega) = 1 + \frac{\chi_d}{1 - (\omega/\omega_0)^2 + (j\omega/\omega_r)^v} \quad (4)$$

where ω is the angular frequency which is equal to $2\pi f$, $\nu \in (0,1)$ is a dispersion parameter and ω_0 is angular frequency, when the walls are oscillating at resonance. The relaxation frequency ω_r is reciprocal to the relaxation time T , $\omega_r = 1/T$. The χ_d is initial susceptibility of d.w. motion. The first dispersion of $\mu'(f)$ (Fig. 3a) due to domain wall resonance oscillation is superimposed with the relaxation of domain wall and may be fitted by the real part of (4). Therefore, the frequency value corresponding to maximum of absorption (losses) does not correspond to the zero of $\mu'(f)$. It is seen from Fig. 3b, that data of the permeability locus may be fitted by (4) and they have a tendency to approach to circular arc indicating resonance behaviour starting at 7 MHz, and influenced by relaxation effects at this lower frequency. In the high frequency region, 0.09 - 0.9GHz, one can assume that walls of grains are sequential pinned, having their own amplitude and relaxation frequency. Then, this part of first locus implies the relaxation behaviour. In this frequency region, the permeability may be fitted by corrected (5) to pure Cole-Cole relaxation character as follow

$$\tilde{\mu}_d(\omega) = \frac{\chi_d}{1 + (j\omega/\omega_r)^v} \quad (5)$$

In frequency region higher than 0.9 GHz, the second resonance dispersion of permeability spectra is started.

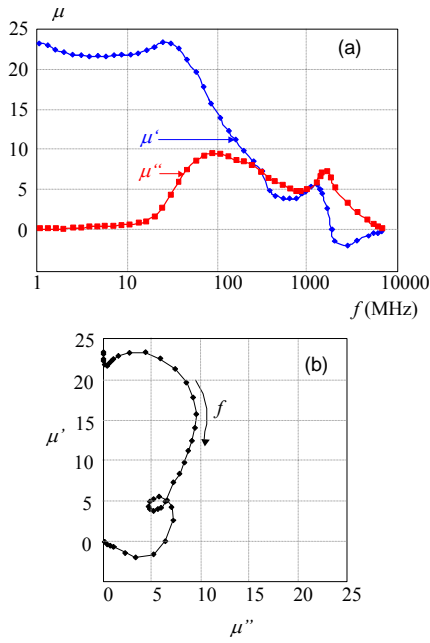


Fig. 3. Frequency spectra of NiFe₂O₄ ferrite: (a) - real μ' and imaginary μ'' components, (b) - complex permeability μ^*

The explanation of this resonance is based on a Landau-Lifshitz idea, that crystalline anisotropy is equivalent to an effective static magnetic field H_{ef} , acting inside each crystallite, and that H_{ef} produces a Larmor precession of the appropriate electron spins. At higher frequencies (above 0.9 GHz) the data are consistent with part of circular arc locus in the first approximation, see Fig. 3b. In the highest frequencies the locus indicates practically resonance character with frequency $f_{0S} \approx 1.8$ GHz and there the $\mu'(f)$ corresponds to zero. The last part of locus can be fitted by equation

$$\begin{aligned} \mu_s^*(\omega) &= 1 + \chi_s^*(\omega) = \\ &= 1 + \frac{(\omega\omega_{os}\alpha + j\omega_{os}^2)\chi_{is}}{2\omega\omega_{os}\alpha + j[\omega_{os}^2 - (1+\alpha)\omega^2]} \end{aligned} \quad (6)$$

where α is damping parameter of motion of the magnetization. Derivation of (6) was based on Kittel consideration the ferromagnetic spin resonance, but instead of an ellipsoidal sample, the spherical one was used and damping factor was not neglected. For a polycrystal containing randomly oriented crystallites, Snoek found by means of an averaging calculation the angular resonance frequency due to domain rotations, ω_{os} , given by formula

$$\omega_{os} = \gamma(M_s / \chi_{is})(2/3) \quad (7)$$

where γ is the magneto mechanical ratio, M_s is spontaneous magnetization and initial rotation susceptibility is

$$\chi_{is} = \mu_0 M_s^2 / 3K \quad (8)$$

The first anisotropy constant K plays here important role. The true resonance frequency can be estimated if real part of $\chi_s^*(\omega)$ in (6) will be given zero, $\chi_s'(\omega)=0$. Thus the

measure (true) resonance frequency ω_{os}' is to be compared with the theoretical precession frequency and we obtain

$$\omega_{os}' = 2\pi f_{os}' = \frac{\omega_{os}}{(1 + \alpha^2)^{1/2}} \quad (9)$$

The ferrite composite materials were made by mixing the Ni_{0.36}Zn_{0.64}Fe₂O₄ ferrite particles with appropriate amounts of PVC and pressing the mixture into toroidal form [5]. Several samples with various ferrite filler volume concentration κ_v were prepared and magnetic spectra were measured.

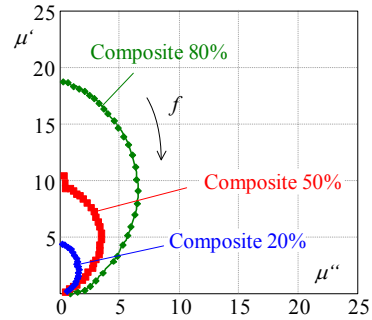


Fig. 4. Frequency spectra of complex permeability μ^* for composite with $\kappa_v=80, 50, 20$ vol %, $f=1$ MHz - 3GHz

The average diameter of ferrite particles $\langle D \rangle = 250 \mu\text{m}$ was used. Series of the samples was prepared to examine the effect of the ferrite content on the permeability spectra. Experimental data of complex permeability of ferritepolymer samples are plotted by three sets of the complex plane loci in Fig. 4 for ferrite particle contents $\kappa_v=80, 50$ and 20 vol %. The composites have simple frequency spectra $\mu^*(f)$ showing only one dispersion due to relaxation process.

4 FREQUENCY SPECTROSCOPY OF FERRITEPOLYMER

In the ferritepolymer composites, the non-magnetic matrix cuts of intrinsic magnetic properties of particles as a result of changes the internal magnetic field in the composite. Therefore, compared with sintered ferrites, ferritepolymers are characterized by a different dispersion of permeability [6,7,8]. The surface of ferrite particle has irregular structure. The porosity parameter has been used to the study the behaviour of ferrites and ferritepolymer composites. The intragranular porosity plays the same role in both the sintered ferrites and the composites. It results in drastic decreasing of the initial permeability. In ferrites the intergranular porosity plays higher role compared with sintered ferrites. The particle size and total porosity cause the demagnetizing field, which increase when filler concentration decreases. The demagnetizing field led to the pinning the domain walls in particles and hence, to the breaking of domain wall motion under an alternating external field. Thus the magnetization rotation mechanism carries out rather than domain wall motion in studied NiZn ferritepolymers.

In the case of magnetization (spin) relaxation, we dealt with the special case of alternating field applied in a plane perpendicular to a projection of effective field corresponded with total magnetic anisotropy. Because of the precessional behaviour, a finite time is required for the magnetization to align itself with projection of H_{ef} , characterized by relaxation time T_s . This means that alternating magnetization will lag behind the applied field. For this relaxation-type of magnetization (spin) rotation mechanism the permeability equation can be estimated by this relation

$$\mu_{os}^* = 1 + \frac{\chi_{is}}{1 + (j\omega T_s)^v} \quad (10)$$

where T_s is the relaxation time of rotation mechanism. In Fig. 4, the measured loci can be fitted by (10) and they are parts of circular arcs or Cole-Cole flattened half-circle diagrams. The loci have higher values of $\mu^*(f)$ for higher filler concentration κ_v .

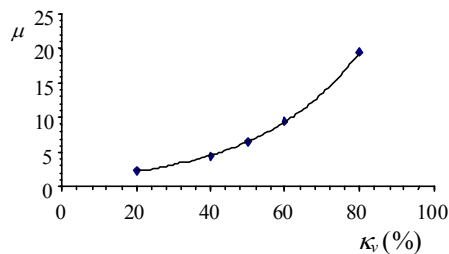


Fig. 5. Low frequency permeability dependence as a function of filler concentration κ_v in ferritepolymers

Variation of the real part permeability μ' measured at low frequency ($f \rightarrow 0$) is increasing with the ferrite volume concentration κ_v , Fig. 5. It can be explained by the decreasing the total anisotropy given by the magneto crystalline one, but mainly by magnetic interactions associated with demagnetizing field decreasing.

In addition, the relaxation frequency f_r is roughly inversely proportional to κ_v . The relaxation frequency $\omega_{rs} = 1/T_s$ due to domain rotation can be derived from (7) and (8) as

$$f_{rs} = -\frac{\gamma\alpha M_s}{2\pi\chi_{is}} = \frac{1}{2\pi} \frac{\gamma\alpha M_s}{\mu - 1} \quad (11)$$

Dependence of relaxation frequency f_r on reciprocal of permeability $1/\mu$ is depicted in Fig. 6, there is roughly linear dependence. This dependence can be fitted by (11) and it can serve as proof as indication of the natural rotating magnetization in ferritepolymers.

5 CONCLUSION

The dielectric and magnetic relaxation or resonance spectroscopy was showed as a powerful technique for the study of polarization or magnetization mechanism and dispersion or absorption of permittivity/permeability in investigated magnetic dielectrics

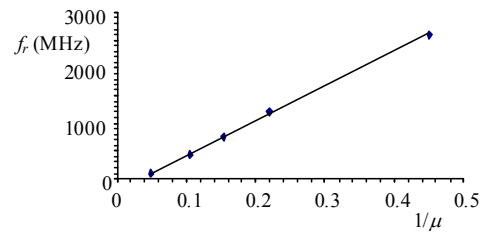


Fig. 6. Relaxation frequency f_r dependence as a function of inverse value of permeability $1/\mu$

The ferrite polymer manifest itself as magnetic media with the reduction of low frequency permeability, but on the other hand, having acceptable value of permeability in higher frequency region compared with NiZn and Li sintered ferrite. It has also very low losses in the high frequency region. Compared with sintered NiZn and Li ferrites, the NiZn ferritepolymer composites is perspective for application in a range high frequency. The magnetization rotation mechanism can be attributed to ferritepolymer magnetization for all filler concentrations. This opinion is due to that, the character of relaxation frequency dependence versus inverse value of permeability has linear behaviour and can serves as a proof of the indication of the natural rotating magnetization in ferritepolymers. From theoretical point of view, one can find two magnetic dispersion and absorption in the Ni ferrite. They attributed the first dispersion to the domain wall resonance superimposed with relaxation, and the second one, at higher frequencies, to the spin resonance. In addition its $\mu^*(f)$ spectra are analogical to Maxwell-Wagner effect of dielectric in first approximation. On the other hand, one can admit idea, that $Ba_{0.25}Sr_{0.75}$ ferrites have two dielectric relaxation dispersion and absorption, which are formed as Maxwell-Wagner effect.

Acknowledgement

This work has been supported by VEGA - Slovak Republic, under projects No. 1/4086/07 and 1/0575/09.

REFERENCES

- [1] SLÁMA, J. - DOSOUDIL, R. - UŠÁKOVÁ, M. - UŠÁK, E. - GRUSKOVÁ, A. - JANČÁRIK, V.: J. Magn. Mater. **304**, e758 (2006)
- [2] GRUSKOVÁ, A. - JANČÁRIK, V. - SLÁMA, J. - DOSOUDIL, R.: J. Magn. Mater. **304**, e762 (2006)
- [3] UŠÁKOVÁ, M. - LUKÁČ, J. - DOSOUDIL, R. - JANČÁRIK, V. - GRUSKOVÁ, A. - UŠÁK, E. - SLÁMA, J. - ŠUBRT, J.: J. Mat. Sci.: Mat. in Electr., **18**, 1183 (2007)
- [4] GLOBUS, A.: J. Phys. Suppl. C1/Proc. ICF-3/C1-C15 (1977)
- [5] DOSOUDIL, R. - OLAH, V.: J. El. Eng. **52**, 1-2, 24 (2001)
- [6] MOHAMED, E. M. et al.: Mat. Res. Bull. **37**, 753 (2002)
- [7] Singh, P. et al.: J. Appl. Phys. **87**, 4362 (2000)
- [8] ZHANG, X. Y. et al., Mat. Lett. **1**, 4332 (2003)

